ENGINEERING RESEARCH JOURNAL (ERJ)

Vol. 1, No. 48 Apr. 2021, pp 1-7

Journal Homepage: http://erj.bu.edu.eg

Statistical Analysis of Friction Stir Welding Parameters

Mohamed F. Sakr *, R. M. Afify, A. M. Gaafer, E. H. Mansour.

"Department of Mechanical Engineering, faculty of Engineering at Shoubra, Benha University, Egypt"

Abstract

In this study, the influence of friction stir welding process variables were investigated using analysis of variance and responses surface method (RSM). Micro/macro-structure, tensile strength, hardness and bending strength were examined to ensure welding joints soundness conformed to required specification. FSW was conducted with three different rotational speeds 800, 450 and 230 rpm: and three different traverse speed of 20, 40 and 60 mm/min. The tool pin profiles that were used for this study (threaded taper profile, tapered profile and cylindrical profile). An Aluminum alloy AA6063 was used as distinctive materials. Then, the root cause analysis was applied to restrict the defects and defects reason. Finally, the result of macro-microstructure study was helped to distribute the defects according to defect size discovered. The results provide that 83.33% of the defects are controlled by 43% of the root causes.

KEYWORDS: Friction Stir Welding, (ANOVA), (RSM), Aluminum alloy

1. Introduction

The aims of this work to study the effect of variation of processing variables (tool rotation speed, tool pin profile and traverse speed) on macro and microstructure of friction stir welding process of 6063 Al alloy. The unprocessed and processed regions will be compared on the basis of their defect's analysis, microstructural and mechanical properties. The study carried out by LORRAIN O. et al. [1] led to an attempt to understand the path of the material flow process resulting from the axial rotational movement of the welding tool using friction stir welding, and it was concluded that the shape and design of the welding tool have the greatest impact on the flow of heat, materials and formation Welding area and its characteristics. On the other hand, LIU H. J. et al. [2]. have studied the tensile properties and places where cracking defects occur in the welded joints, they have used friction stir welding of aluminum alloys and they have concluded that the tensile strength and cracking properties depend on the shape of welding tool foremost, then other input parameters. The study carried out by SABARI SS et al. [3] to study the effect of pin cross section shape on fine structure, mechanical properties for welded joints of aluminum alloy, using friction stir welding process. They have proven that the welding tool plays an influential role on the properties of welded joints. In addition, they have determined the important welding parameters and the appropriate dimensions of the welding tool. Additionally, ELANGOVAN K. et al. [4] have determined three different welding tool diameters and applied friction stir welding on aluminum alloy (AA6061) in order to determine the relationship between the dimensions of the welding tool and the mechanical properties of the welded joints. Similarly, ARORA A. et al. [5] have studied the relationship between the welding tool and the characteristics resulting from the change in the shape pin profile of the welding tool. they were concluded that an increase in the shoulder diameter leads to an increase in the temperature resulting from an increase in the surface area of friction. It was also found that a tool whose adhesion torque corresponds to the diameter of the shoulder improves the tensile strength of welded samples. The study conducted by WANG KUUI SHE et al. [6] to connect the different welding joints of aluminum alloys under varying conditions of welding speed and pin depth of welding tool. they have found that, the pin of the welding tool has controlled in the area and the flow pattern of welding material. They have also found that the shape and design of the pin had a great role in reducing the forging force during the immersion of the pin in the material. WANG Q. et al. [7] have been concerned with improving the strategy of welding parameters so that the welded joints resulting from the welding process are free from defects. In their experiments on several alloys, using friction stir welding to connect these joints. They have reached the discovery of a group of defects resulting from this

process such as (voids, grooves, tunnels, kissing bond). Defects are generally caused by improper heating rate resulting from wrong welding parameters.

2. Experiment Procedure

2.1 Materials and welding machine:

In this investigation, aluminum alloy (AA6063) was chosen. The advance RF-40HC GEARD head floor type milling drilling machine was used as friction welding machine.

2. 2 Design of welding tools:

A high-speed steel rod of 20Ø mm and 100 mm length was used with dimensions of 20mm shoulder length, 16mm shoulder diameter and 4.5mm pin length. Three different pin profile of welding tool (cylindrical, tapered, and threaded taper) were used.

2.3 Design of experiment:

In this study, the response surface is designed for three factors as shows in table 2.1. The Design Expert 11 program was used for the analysis to improve the mechanical properties of the friction stir welding joints. The responses are hardness, bending resistance, and tensile strength.

Factor	Name	Units	Level 1	Level 2	Level 3
A	Tool Rotational Speed	rpm	230	450	800
B	Tool Traverse speed	mm/min	20	40	60
C	Pin profiles		Cylindrical	Tapered	Taper Threaded

Table 2.1 Critical parameters and levels.

2.4 Destructive tests:

Welded coupons were tested with DynaROCK ll device. Three points were selected on center line of the seam weld for each specimen. The hardness average was calculated of these points that was measured in the scale B by the method HR (Hardness Rockwell). The tensile strength test specimens were processed according to B557 – 10 Standard [8]. The universal hydraulic test machine was use for the both tensile and bending tests.

3. Results and Discussion

3.1 Response surface and optimization modeling:

In this part, the results of experiments and statistical analysis of the relationship between inputs and outputs are presented and discussed. Table 3.1 shows the experimental data for all factors and measured responses. The statistical analysis described in this study was used of affects the analysis of variance (ANOVA), adjusted R2. The design of expert software was used to realization general trends and impacts.

A series of steps were followed (Response surface > Factorial > Analyze Factorial Design) to analyze factorial design the results as well as to generate the ANOVA table for the experiment, regression equations and graphs that help to communicate the results and determine how parameters affect the response factors (hardness, tensile strength and bending strength).

TABLE 3.1 Experimental Data.

Run	A: Tool Rotational Speed	B: Tool Traverse speed	C: Pin profiles	Hardness	Tensile strength	Bending strength
	rpm	mm/min		Rockwell	N/mm2	N/mm2
1	800	40	T	30.289	78.464	131.929
2	230	60	C	27.249	49.853	136.374
3	450	40	C	25.088	45.713	127.827
4	450	60	T	24.716	44.064	152.462
5	450	20	T	26.784	58.848	106.485
6	450	60	TT	28.236	51.937	159.394
7	230	40	TT	31.886	70.248	140.566
8	230	40	TT	32.51	73.507	139.8
9	450	40	C	24.414	39.228	125.768
10	800	20	C	24.899	47.976	107.464
11	450	20	TT	28.19	58.264	126.887

12	800	40	TT	29.402	65.864	142.143
13	450	40	T	25.565	42.903	141.036
14	230	20	C	29.489	64.639	107.57
15	230	20	T	27.246	54.168	107.129
16	800	20	TT	29.597	68.464	134.895
17	230	20	TT	32.013	74.936	121.309
18	450	40	C	24.645	39.205	124.698
19	800	20	T	30.072	79.492	113.153
20	450	60	TT	28.892	54.883	150.866
21	800	60	C	26.764	57.686	142.007
22	450	60	T	25.566	44.914	153.312

The analysis of variance for reduced quadratic model for hardness was given the Predicted R^2 of 0.9014 was in reasonable agreement with the Adjusted R^2 of 0.9530 as shown in table 3.2. The factors C, AB, AC, A^2 are significant model terms. The analysis for tensile strength was given the Predicted R^2 of 0.8266 is in reasonable agreement with the Adjusted R^2 of 0.9210. .

The factors A, B, C, AB, AC, A^2 are significant model terms as shown in table 3.3. Finally, the analysis of variance for reduced quadratic model for bending strength was given the Predicted R^2 of 0.9150 is in reasonable agreement with the Adjusted R^2 of 0.9433. The factors B, C, BC are significant model terms as shown in table 3.4

Table 3.2 ANOVA for hardness.

Source	Sum of Squares	df	Mean Square	F-value	p-value	
Model	3278.44	8	409.81	31.60	< 0.0001	significant
A-Tool Rotational Speed	101.20	1	101.20	7.80	0.0152	
B-Tool Traverse speed	100.11	1	100.11	7.72	0.0157	
C-Pin profiles	825.82	2	412.91	31.84	< 0.0001	
AB	122.89	1	122.89	9.48	0.0088	
AC	655.08	2	327.54	25.25	< 0.0001	
A^2	744.16	1	744.16	57.38	< 0.0001	
Residual	168.60	13	12.97			
Lack of Fit	130.46	8	16.31	2.14	0.2093	not significant
Pure Error	38.15	5	7.63			
Cor Total	3447.04	21				

Table 3.3 ANOVA for tensile strength.

Source	Sum of Squares	df	Mean Square	F-value	p-value	
Model	5271.34	6	878.56	59.22	< 0.0001	significant
A-Tool Rotational Speed	57.22	1	57.22	3.86	0.0684	
B-Tool Traverse speed	4177.34	1	4177.34	281.57	< 0.0001	

C-Pin profiles	1140.34	2	570.17	38.43	< 0.0001	
BC	192.29	2	96.14	6.48	0.0094	
Residual	222.54	15	14.84			
Lack of Fit	180.46	10	18.05	2.14	0.2068	not significant
Pure Error	42.08	5	8.42			
Cor Total	5493.87	21				

TABLE 3.4 ANOVA for bending strength.

Source	Sum of Squares	df	Mean Square	F-value	p-value	
Model	133.41	8	16.68	54.26	< 0.0001	significant
A-Tool Rotational Speed	0.9952	1	0.9952	3.24	0.0952	
B-Tool Traverse speed	0.3117	1	0.3117	1.01	0.3322	
C-Pin profiles	53.77	2	26.89	87.48	< 0.0001	
AB	2.92	1	2.92	9.50	0.0088	
AC	20.35	2	10.18	33.11	< 0.0001	
A^2	27.52	1	27.52	89.54	< 0.0001	
Residual	4.00	13	0.3073			
Lack of Fit	2.99	8	0.3737	1.86	0.2566	not significant
Pure Error	1.01	5	0.2011			
Cor Total	137.41	21				

The highest contribution percentage of hardiness model gives 39.13% for pin profile. The highest contribution percentage of tensile model gives 32.96% for pin profile. Finally, the contribution percentage of bending strength model gives 76.04% for traverse speed followed by 20.76% for pin profile. The method was used to validate the models. Where, x^2 of 0.1430 was measured for hardness model, x^2 of 3.2448 for tensile strength model and x^2 of 1.6887 for bending strength model. Chi-square was measured at significance level of 0.01, and DOF of 21. The chi-square values of all models were less than critical value of 38.932. The variables were independent (accepted null hypothesis). So that, the 99.9% of the variability in the hardness, tensile and bending was explained by these models.

3.2 Macro and micro structural tests:

This study viewed the grains growth of welded area, HAZ and the base metal. The investigation tests were taken only for those samples which have highest and lowest average values of the mechanical properties of each type of pin profiles. The Olympus BX51M metallurgical microscope at magnification of 10X to as high as 100X was used to study a welding profile.

The discovered defects were distributed as per the defect size as shown in table 3.5. At this part, the study of micro-macro structure was applied on six random samples of 27.27% of 22 lot size and 22 experimental runs. The minimum defects target was less than 30% of the defects ≥ 1mm. The total inspected points were 30 points as a following (7 defects ≥ 1mm and 23 defects ≤ 1mm). The defects ratio was 23.33% ≤ 30%, so that the lot size accepted. The relation between defects and the root causes analyzed by pareto chart as shown in fig 3.1. The class limit and frequency distributed as a following ([0mm-0.2mm = 5 defects], [0.2mm-0.4mm = 12 defects], [0.4mm-0.6mm = 0], [0.6mm-0.8mm = 0], [0.8mm-0.1mm = 6 defects], and [> 1 mm = 7 defects]). Therefore, 43% of the root causes controlled 83.33% of the defects as shown in Fig 3.2.

SN	Run #21	Run #8	Run #1	Run #10	Run #11	Run #15
1	>1 mm void	>1 mm void	>1 mm Tunneling	>1 mm Tunneling	>1 mm	>1 mm Tunneling

Table 3.5 Defects distribution according to defect size discovered.

			defect	defect	void	defect
2	1 mm Tunneling defect	1 mm Tunneling defect	0.2 mm kissing bond defect	>1 mm kissing bond defect	1 mm voids	1 mm Tunneling defect
3	0.2 mm voids	1 mm voids	0.2 mm voids	1 mm Tunneling defect	0.2 mm Pore	0.2 mm voids
4	0.2 Pore	0.2 mm voids	0	0.2 mm voids	0	0.2 mm Pore
5	0.2 kissing bond	0.2 mm Pore	0	0.2 mm Tunneling defect	0	0

The pin depth of welding tool was 4.5 mm and the thickness of Al plate was 6 mm. Therefore, overbalances the resone of tunnel defects were due to small pin depth specially at noticing this type of defects at all test samples. The resultant tunnel defects were appeared because likely some reasons of insufficient heat generation, insufficient metal transportation as shown in fig. 3.4 & 3.5 and due to excess heat input per unit length of the welding joints and without vertical movement as per shown in fig. 3.6 & 3.7. The increased of traverse speed resulted in poor plasticization of metal which was leaded to tunnel defects as shown in fig. 3.3 & 3.4. The most reasons of voids defects were increased in turbulence of the plasticized metal due to uncontrollable vibration on the milling machine shaft and vibrated welding tool as shown in fig. 3.7 and 3.8. Insufficient stirring surface leaded to directly bonded without the metallic bond between oxide free surface in the root part of the welding joints as shown in 3.8 & 3.6.

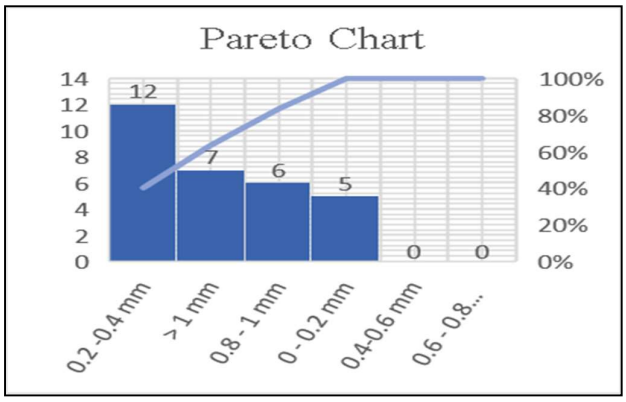

Fig. 3.1 Pareto chart.

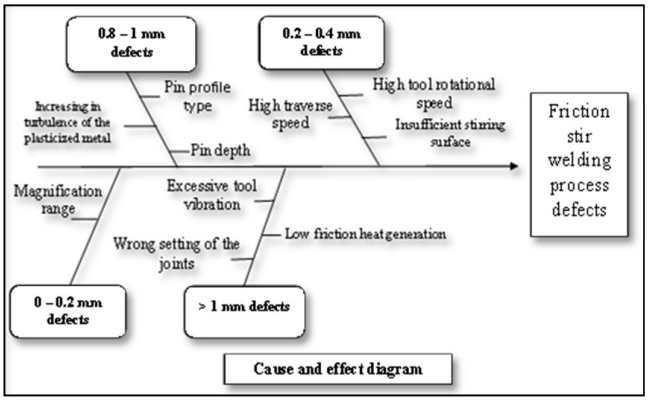

Fig. 3.2 Defects root cause analysis for FSW applied on Al 6063 alloy.

Fig. 3.3 Macro/Micrographs of the surface of friction stir welding sample for cylindrical pin profile (run # 21).

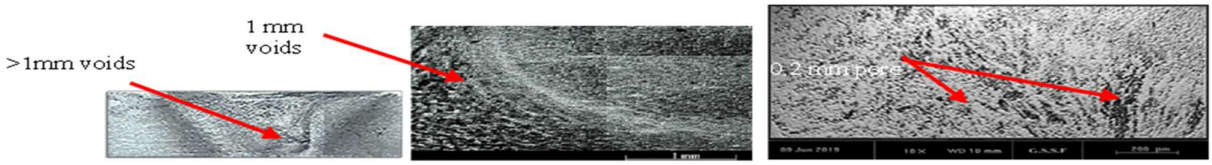

Fig. 3.4 Macro/Micrographs of the surface of friction stir welding sample for threaded taper pin profile (run # 8).

Fig. 3.5 Macro/Micrographs of the surface of friction stir welding sample for taper pin profile (run # 1).

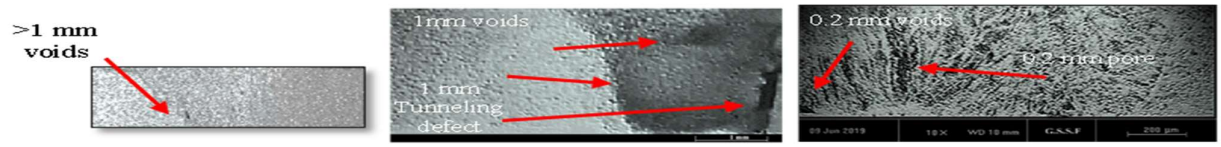

Fig. 3.6 Macro/Micrographs of the surface of friction stir welding sample for cylindrical pin profile (run # 10).

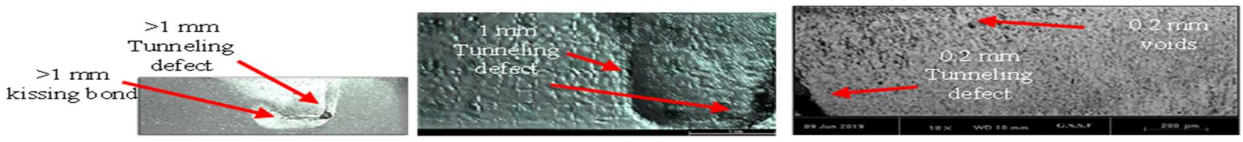

Fig. 3.7 Macro/Micrographs of the surface of friction stir welding sample for threaded taper pin profile (run # 11).

Fig. 3.8 Macro/Micrographs of the surface of friction stir welding sample for taper pin profile (run # 15).

Conclusion

1. Threaded pin profile has given the maximum hardness followed by threaded taper profile followed by cylindrical profile. Threaded taper pin profile was given the maximum tensile strength followed by tapered profile followed by cylindrical profile. Threaded taper pin profile was given the maximum bending strength followed by taper profile followed by cylindrical profile.
2. The maximum contribution percentage of traverse speed = 76.04% for the bending strength model followed by pin profile that was 39.13% for the hardness model. Then, pin profile was 32.96% for the tensile strength model.
3. The analysis has shown the 83.33% of the defects are controlled by 43% of the root causes.

References:

1. LORRAIN O, FAVIER V, ZAHROUNI H, LAWRJANIEC D. Understanding the material flow path of friction stir welding process using unthreaded tool [J]. Journal of Material Processing Technology, 2010, 210: 603-609.

2. LIU H J, FUJII H, MAEDA M, NOGI K. Tensile properties and fracture locations of friction stir welded joints of 6061-T6 aluminum alloy [J]. Materials Science Letters, 2003, 22: 1061-1063.
3. SABARI S S, MALARVIZHI S, BALASUBRAMANIAN V, REDDY G. The effect of pin profiles on the microstructure and mechanical properties of underwater friction stir welded AA2519-T87 aluminum alloy [J]. International Journal of Mechanical and Materials Engineering, 2016, 11(5): 1-14.
4. ELANGOVAN K, BALASUBRAMANIAN V. Influences of tool pin profile and tool shoulder diameter on the formation of friction stir processing zone in AA6061 aluminum alloy [J]. Materials and Design, 2008, 29(2): 362-373.
5. ARORA A, DE A, DEBROY T. Toward optimum friction stir welding tool shoulder diameter [J]. Scripta Materialia, 2011, 64(1): 9-12.
6. WANG Kuai-she, WU Jia-lei, WANG W, ZHOU Long-hai, LIN Zhao-xia, KONG Liang. Underwater friction stir welding of ultrafine grained 2017 aluminum alloy [J]. Journal of Central South University, 2012, 19: 2081-2085.
7. WANG Q, ZHAO Z, ZHAO Y, YAN K, ZHANG H. The adjustment strategy of welding parameters for spray formed 7055 aluminum alloy underwater friction stir welding joint [J]. Materials and Design, 2015, 88: 1366-1376.
8. ASTM International, 100 Barr Harbor Drive, PO Box C700, West Conshohocken, PA 19428-2959, United States. Individual reprints (single or multiple copies) of this standard may be obtained by contacting ASTM at the above address or at 610-832-9585 (phone), 610-832-9555 (fax), or service@astm.org (e-mail); or through the ASTM website (www.astm.org).
9. TWI Ltd. “The bend test is a simple and inexpensive qualitative test that can be used to evaluate both the ductility and soundness of a material”. Granta Park, Great Abington, Cambridge, CB21 6AL, UK. (contactus@twi.co.uk).